Supplementary Information (SI) for Nanoscale.
This journal is © The Royal Society of Chemistry 2026

Supplementary Information

Nanowire photodetectors: Path to single physical artificial neurons

Yunqiu Chen, Milad Fathabadi, Mohammad Fazel Vafadar, and Songrui Zhao

Department of Electrical and Computer Engineering, McGill University, 3480 University Street, Montreal, Quebec H3A 0E9, Canada

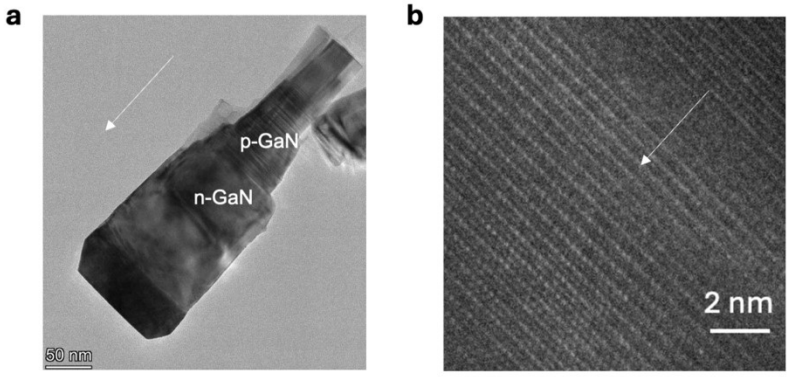

Extended Data Fig. 1 | Additional electron microscopy images. a, A low-magnification TEM image. **b**, HRTEM highlighting the n-GaN/n-AlGaN interface.

Supplementary Note 1 | Additional electron microscopy studies

In the present study, the n-GaN and p-GaN segments can be distinguished by the Mg doping induced stacking faults, as shown in Extended Data Fig. 1a. Extended Data Fig. 1b shows an exemplary high-resolution transmission electron microscopy (HRTEM) image for the n-GaN/n-AlGaN interface, and crystalline planes can be clearly seen.

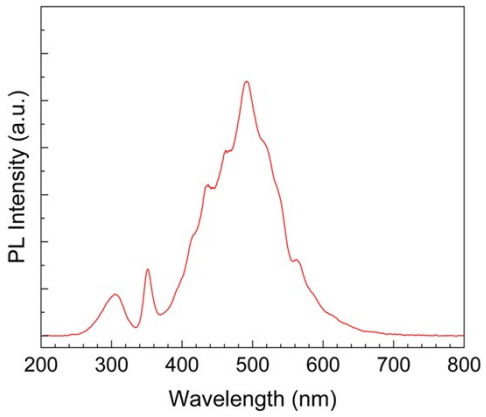

Extended Data Fig. 2 | RTPL spectrum of the light-detecting PNNP nanowires. The structural detail can be found in the main text.

Supplementary Note 2 | Alloy composition of the light-detecting nanowires

In this study, the In and Al contents were estimated based on the room-temperature photoluminescence (RTPL) measurements, which were performed using a 213 nm pulsed laser. During the experiments, the laser was focused onto the sample surface. The emitted light was collected with a lens which is coupled to an optical fiber connected to a UV - visible spectrometer. More details can be found in Refs. [1,2].

As shown in Extended Data Fig. 2, RTPL peaks centered around 500 nm (~ 2.5 eV) and 300 nm (~ 4.1 eV) are measured, corresponding to the InGaN and AlGaN layers, respectively. This indicates that the InGaN layer has an optical bandgap of around 2.5 eV, corresponding to an In mole fraction of 0.26, i.e., $In_{0.26}Ga_{0.74}N$. On the other hand, the AlGaN layer has an optical bandgap of 4.1 eV, which corresponds to an Al mole fraction of 0.3 [1,2]. The bumps on the shoulder of the 500 nm RTPL peak could be due to In content inhomogeneity, which has been commonly observed in InGaN semiconductors [3-6].

The RTPL peak at 350 nm could have several contributions, including near-band-edge exciton emission of GaN [7-10], defect emission from the doped AlGaN [11], Al content inhomogeneity in the AlGaN layer [12,13], or AlN defect emission from the AlN shell [14,15].

A clear GaN RTPL is not observed in the present study. Nonetheless, it does not mean there is no UV light absorption by GaN. As the excitation laser light is strong, it can be scattered to the nanowire root and absorbed by GaN. However, GaN RTPL could be much weaker and absorbed by the top p-InGaN layer.

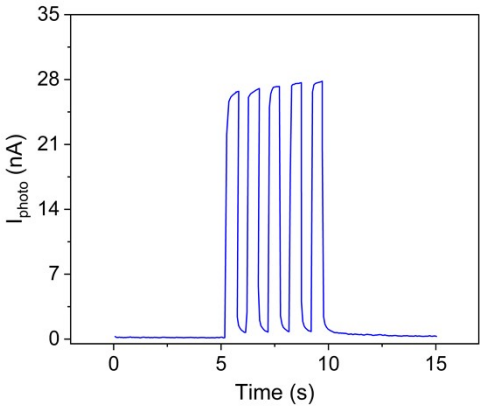

Extended Data Fig. 3 | The time-dependent photocurrent from the comparison structure (PNP) under the UV light illumination. The light average power density was 3 mW·cm^{-2} and the applied bias was 0.4 V. Due to the removal of the charge trap, the temporal summation of the positive photocurrent is absent even at an applied bias of 0.4 V.

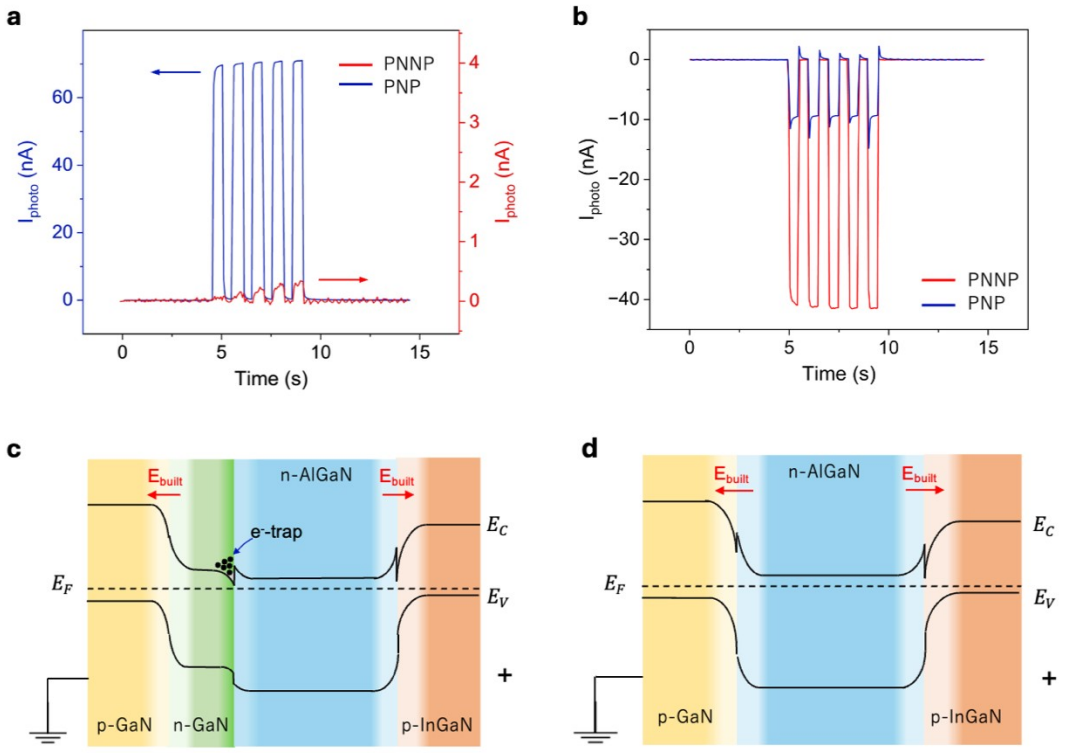

Extended Data Fig. 4 | Time-dependent photocurrent for PNNP and PNP structures. a, **b**, Photocurrent versus time for the PNNP and PNP structures under 0 V and excited by the UV and

blue light, respectively. The average light intensity for the UV light is 9 $mW \cdot cm^{-2}$ and for the blue is 0.52 $W \cdot cm^{-2}$. **c**, **d**, Energy band diagram for PNNP and PNP structure, respectively.

Supplementary Note 3 | Detailed comparison with the reference PNP structure

In this study, the charge trapping effect at the n-GaN/n-AlGaN interface is also examined by the comparison nanostructure (PNP), wherein the n-GaN layer between p-GaN and n-AlGaN is removed (and thus the charge trap is removed). In this case, it is expected that the temporal summation of the positive photocurrent under the UV light illumination would disappear. This is indeed the case as what we have observed. Namely, when the light is turned off, the photocurrent drops rapidly to zero, and no persistent positive photocurrent; and when the light is turned back on, the photocurrent restores the previous value (rather than increasing). The time-dependent photocurrent in this case can be found in Extended Data Fig. 3.

Moreover, for the PNP reference structure, under the UV light illumination at zero bias, a net positive photocurrent is measured. This could be due to effects such as the larger band offset at the n-AlGaN/p-InGaN interface compared with the n-AlGaN/p-GaN interface and presumably better absorption of UV light from the n-GaN layer due to a larger thickness.

The effect of removing the n-GaN layer can also be seen in Extended Data Fig. 4a, which shows the photocurrent under the UV light illumination at zero volt applied bias for the two structures. It is seen that the PNP structure has a much higher positive photocurrent. This could be mainly due to the presence of the electron trap at the n-GaN/n-AlGaN interface in the PNNP structure and a smaller electric field at the p-GaN/n-GaN interface in the PNNP structure compared to that at the p-GaN/n-AlGaN interface in the PNP structure.

On the other hand, the stronger electric field at the p-GaN/n-AlGaN interface (PNP structure) compared to that at the p-GaN/n-GaN interface (PNNP structure) could undermine the negative photocurrent under the blue light illumination at zero volt applied bias, and this is the case as shown in Extended Data Fig. 4b.

Supplementary Note 4 | More discussions on the photocarrier dynamics

In photodetection based on p-n junction semiconductors, the output photocurrent is proportional to how efficiently photogenerated electron-hole pairs are separated and extracted from the semiconductor. Typically, a stronger E-field at the p-n junction interface leads to better charge separation and thus higher photocurrent.

The comparison of the E-field strength for the p-GaN/n-AlGaN (pN) and the p-GaN/n-GaN (pn) can be estimated using Extended Data Eq. 1, where ε_r is the relative permittivity, x_n is the depletion width inside the n-type semiconductor, and V_{bi} is the built-in voltage of the junction. This equation is derived by assuming doping concentration of ~ 10^{18} cm^{-3} for all semiconductors and taking ε_r for both GaN and AlGaN to be nearly the same. V_{bi} is calculated from Extended Data Eq. 2 and Extended Data Eq. 3, considering an intrinsic carrier concentration (n_i) of ~ 10^{16} cm^{-3} [16], and the effective density of states for the conduction band (N_C) of 2.3×10^{18} cm^{-3} for GaN and 3.5×10^{18} cm^{-3} for AlGaN [16], respectively. The n_{n0} and n_{p0} are the electron concentrations in the n-type and the p-type semiconductor, respectively. The conduction band offset (Δ^{E_c}) of the p-GaN/n-AlGaN is estimated ~ 0.55 eV [17,18].

$$\frac{E_{pN}}{E_{pn}} = \frac{\varepsilon_r^{AlGaN}}{\varepsilon_r^{GaN}} \times \frac{x_n^{AlGaN}}{x_n^{GaN}} \sim \left(\frac{V_{bi}^{pN}}{V_{bi}^{pn}}\right)^{\frac{1}{2}} \sim 1.8 \qquad (Eq.1)$$

$$eV_{bi}^{pN} = \Delta E_C + 0.026\ eV \times \ln\left(\frac{n_{n0}}{n_{p0}} . \frac{N_{cp}}{N_{cN}}\right) \sim 0.77\ eV \qquad (Eq.2)$$

$$eV_{bi}^{pn} = 0.026\ eV \times \ln\left(\frac{N_a N_d}{{n_i}^2}\right) \sim 0.23\ eV \qquad (Eq.3)$$

From this estimation, the p-GaN/n-GaN interface (E_{pn}) in the PNNP structure has a weaker E-field than the p-GaN/n-AlGaN interface (E_{pN}) in the PNP structure. This could contribute to lower positive photocurrent in the PNNP structure compared to the PNP structure.

Moreover, in heterojunctions, the band offset at the interface could act as a barrier for the charge carrier transport, which could further lower the photocurrent. This contributes to the lower positive photocurrent observed in the PNNP structure compared to that in the PNP structure as well when the electron trap is "placed" strategically. Due to the traps of electrons, the positive current due to the electron transport is reduced; in the meantime, the trapped electrons will also combine with photogenerated holes and thus reduce the hole transport, further reducing the positive current.

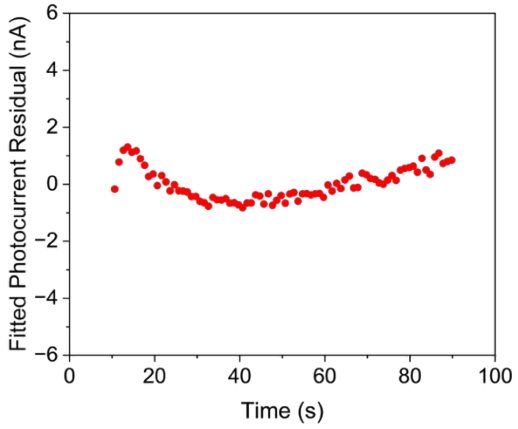

Extended Data Fig. 5 | Residual photocurrent from the fitting. The details of fitting are discussed in the main text. A small residual magnitude and no obvious trend of the data indicate an excellent fitting quality.

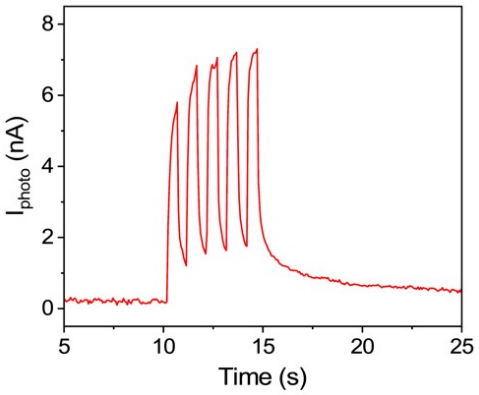

Extended Data Fig. 6 | Time-dependent photocurrent of a smaller device (300 µm × 300 µm) on the same wafer sample. The curve is obtained with 50 mV bias and 3 mW·cm^{-2} of UV light.

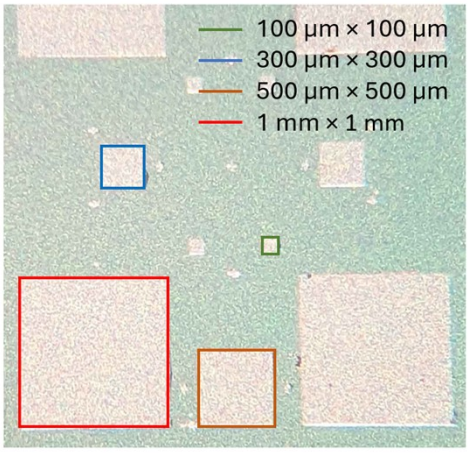

Extended Data Fig. 7 | Microscopic image of a fabricated wafer sample. The metal contact size, which defines the device size, is also denoted.

References

1 Chen, Y. *et al.* Real-Time, Dual-Physical-Layer Encryption Directly within an Optical Sensor on a Silicon Platform. *ACS Appl Mater Interfaces* **17**, 28350-28356 (2025). https://doi.org/10.1021/acsami.5c00535

2 Fathabadi, M., Yin, Y., Li, S. & Zhao, S. Breaking the Built-In Electric Field Barrier in p–n Heterojunction for Self-Powered, Wavelength Distinguishable Photoelectrochemical Photodetectors: Toward Low Power Consumption and Secure Underwater Wireless Sensor Network. *Advanced Optical Materials* (2023). https://doi.org/10.1002/adom.202302372

3 Goodman, K. D. *et al.* Green luminescence of InGaN nanowires grown on silicon substrates by molecular beam epitaxy. *Journal of Applied Physics* **109**, 084336 (2011). https://doi.org/10.1063/1.3575323

4 Guo, W., Zhang, M., Banerjee, A. & Bhattacharya, P. Catalyst-Free InGaN/GaN Nanowire Light Emitting Diodes Grown on (001) Silicon by Molecular Beam Epitaxy. *Nano letters* **10**, 3355-3359 (2010). https://doi.org/10.1021/nl101027x

5 Smith, M. *et al.* Time-resolved photoluminescence studies of InGaN epilayers. *Applied Physics Letters* **69**, 2837-2839 (1996). https://doi.org/10.1063/1.117335

6 Nguyen, H. P. T. *et al.* Engineering the Carrier Dynamics of InGaN Nanowire White Light-Emitting Diodes by Distributed p-AlGaN Electron Blocking Layers. *Scientific Reports* **5**, 7744 (2015). https://doi.org/10.1038/srep07744

7 Reshchikov, M. A. Measurement and analysis of photoluminescence in GaN. *Journal of Applied Physics* **129**, 121101 (2021). https://doi.org/10.1063/5.0041608

8 Okumura, H., Yoshida, S. & Okahisa, T. Optical properties near the band gap on hexagonal and cubic GaN. *Applied Physics Letters* **64**, 2997-2999 (1994). https://doi.org/10.1063/1.111383

9 Paskov, P. P. *et al.* Emission properties of a-plane GaN grown by metal-organic chemical-vapor deposition. *Journal of Applied Physics* **98**, 093519 (2005). https://doi.org/10.1063/1.2128496

10 Kovalev, D. *et al.* Free exciton emission in GaN. *Physical Review B* **54**, 2518-2522 (1996). https://doi.org/10.1103/PhysRevB.54.2518

11 Hyun Kim, J. *et al.* Tracking of Point Defects in the Full Compositional Range of AlGaN via Photoluminescence Spectroscopy. *physica status solidi (a)* **220**, 2200390 (2023). https://doi.org/https://doi.org/10.1002/pssa.202200390

12 Pierret, A. *et al.* Growth, structural and optical properties of AlGaN nanowires in the whole composition range. *Nanotechnology* **24**, 115704 (2013). https://doi.org/10.1088/0957-4484/24/11/115704

13 Himwas, C., den Hertog, M., Dang, L. S., Monroy, E. & Songmuang, R. Alloy inhomogeneity and carrier localization in AlGaN sections and AlGaN/AlN nanodisks in nanowires with 240–350 nm emission. *Applied Physics Letters* **105**, 241908 (2014). https://doi.org/10.1063/1.4904989

14 Nepal, N., Nakarmi, M. L., Lin, J. Y. & Jiang, H. X. Photoluminescence studies of impurity transitions in AlGaN alloys. *Applied Physics Letters* **89**, 092107 (2006). https://doi.org/10.1063/1.2337856

15 Sedhain, A., Lin, J. Y. & Jiang, H. X. Nature of optical transitions involving cation vacancies and complexes in AlN and AlGaN. *Applied Physics Letters* **100**, 221107 (2012). https://doi.org/10.1063/1.4723693

16 SCHUBERT FRED, E. *Light-Emitting Diodes*. (Cambridge University Press, 2003).

17 Yan, Q., Kioupakis, E., Jena, D. & Van de Walle, C. G. First-principles study of high-field-related electronic behavior of group-III nitrides. *Physical Review B* **90**, 121201 (2014). https://doi.org/10.1103/PhysRevB.90.121201

18 Moses, P. G., Miao, M., Yan, Q. & Van de Walle, C. G. Hybrid functional investigations of band gaps and band alignments for AlN, GaN, InN, and InGaN. *The Journal of Chemical Physics* **134**, 084703 (2011). https://doi.org/10.1063/1.3548872